Intercalative G-Tetraplex Stabilization of Telomeric DNA by a Cationic Porphyrin[1]

Ihtshamul Haq,[†,§] John O. Trent,[‡] Babur Z. Chowdhry,[†] and Terence C. Jenkins*[,†]

Contribution from the School of Chemical and Life Sciences, University of Greenwich, Wellington Street, Woolwich, London SE18 6PF, U.K., and Department of Medicine, Division of Hematology/Oncology, University of Alabama at Birmingham, Birmingham, AL 35294-3300

Received May 5, 1998

Abstract: DNA tetraplex ("quadruplex") structures formed from guanine tetrads and significant to the regulation of telomerase activity have recently been shown to be stabilized by interaction with a cationic porphyrin [Anantha, N. V.; Azam, M.; Sheardy, R. D. *Biochemistry* **1998**, *37*, 2709−2714. Wheelhouse, R. T.; Sun, D.; Han, H.; Han, F. X.; Hurley, L. H. *J. Am. Chem. Soc.* **1998**, *120*, 3261−3262]. Porphyrin binding to DNA sequences from the *Oxytricha* and human telomeres and a thrombin-binding aptamer is here examined by isothermal titration calorimetry (ITC) and spectrophotometry under conditions that favor self-assembly to their respective intermolecular or intramolecular tetraplex structures. Analysis of the ITC and optical data reveals (i) saturating porphyrin/tetraplex binding stoichiometries of 1:1, 2:1, and 3:1 for $d(G_2T_2G_2TGTG_2T_2G_2)$, $d(AG_3[T_2AG_3]_3)$, and $[d(T_4G_4)]_4$, respectively, involving near-equivalent sites, (ii) weak binding of only $(0.3-2) \times 10^5\ M^{-1}$ per site, and (iii) no evidence for stepwise complexation in solutions containing K^+ ions. This stoichiometry is maintained in Na^+ solutions, if the tetraplex is stable, but nondegenerate sites are implicated for the 2:1 and 3:1 complexes where the first porphyrin binds with 20−40-fold greater affinity than any subsequent ligand(s). Importantly, the stoichiometries correspond to the number of intervals between successive G-tetrad planes in each tetraplex. The results indicate binding by threading intercalation at each closely similar GpG site, possibly without invoking neighbor exclusion for adjacent sites, rather than through either external electrostatic processes or end-pasted stacking modes. This mechanism is supported by dynamic molecular modeling simulations with two DNA tetraplexes which show that stable intercalated complexes can be realized. A plausible model is developed that accounts for the occupation of adjacent sites, where unfavorable interligand contacts are avoided by phased asymmetric positioning of the porphyrin molecules within each G-tetrad intercalation pocket.

Introduction

The formation of tetraplex or "quadruplex" DNA structures[2,3] from the tandemly repeating guanine clusters (e.g., 5′-TTAGGG in humans) present in the single-stranded telomere segment at the 3′ ends of chromosomal DNA has been suggested as an attractive chemotherapeutic target for new antitumor agents.[4−7] In part, current interest in this DNA stems from the telomerase-inhibiting activity found for K^+ or Na^+ ions and for various tetraplex-binding compounds,[5,7,8] where stabilization of a four-stranded structure is inferred to impede access to the telomeric DNA template necessary for enzyme function. Telomerase has recently been associated with the longevity of most cancer cells, and the processivity of this enzyme may be essential for their immortalization and proliferative potential.[9]

This activity has prompted a structure-based quest for

* Corresponding author: Professor Terence Jenkins, University of Greenwich. Telephone (+044) 181-331-8209. FAX (+044) 181-331-8305. E-mail t.c.jenkins@gre.ac.uk.

† University of Greenwich.

‡ University of Alabama.

§ Present address: Nuffield Department of Clinical Biochemistry, Institute of Molecular Medicine, University of Oxford, Oxford OX3 9DS, U.K.

(1) Abbreviations: DSC, differential scanning calorimetry; H_2TMPyP, 5,10,15,20-tetrakis(1-methyl-4-pyridyl)-21*H*-porphine; ITC, isothermal titration calorimetry; MD, molecular dynamics.

(2) (a) Blackburn, E. H. *Nature* **1991**, *350*, 569−573. (b) Kang, C. H.; Zhang, X.; Ratliff, R.; Moyzis, R.; Rich, A. *Nature* **1992**, *356*, 126−131. (c) Wang, Y.; Patel, D. J. *Structure* **1993**, *1*, 263−282. (d) Aboul-el, F.; Murchie, A. I. H.; Norman, D. G.; Lilley, D. M. J. *J. Mol. Biol.* **1994**, *243*, 458−471. (e) Laughlan, G.; Murchie, A. I. H.; Norman, D. G.; Moore, M. H.; Moody, P. C. E.; Lilley, D. M. J.; Luisi, B. *Science* **1994**, *265*, 520−524. (f) Phillips, K.; Dauter, Z.; Murchie, A. I. H.; Lilley, D. M. J.; Luisi, B. *J. Mol. Biol.* **1997**, *273*, 171−182.

(3) Wellinger, R. J.; Sen, D. *Eur. J. Cancer* **1997**, *33*, 735−749.

(4) (a) Raymond, E.; Sun, D.; Chen, S.-F.; Windle, B.; Von Hoff, D. D. *Curr. Opin. Biotechn.* **1996**, *7*, 583−591. (b) Salazar, M.; Thompson, B. D.; Kerwin, S. M.; Hurley, L. H. *Biochemistry* **1996**, *35*, 16110−16115. (c) Perry, P. J.; Kelland, L. R. *Expert Opin. Ther. Patents* **1998**, *8*, 1567−1586.

(5) (a) Sun, D.; Thompson, B.; Cathers, B. E.; Salazar, M.; Kerwin, S. M.; Trent, J. O.; Jenkins, T. C.; Neidle, S.; Hurley, L. H. *J. Med. Chem.* **1997**, *40*, 2113-2116. (b) Perry, P. J.; Gowan, S. M.; Reszka, A. P.; Polucci, P.; Jenkins, T. C.; Kelland, L. R.; Neidle, S. *J. Med. Chem.* **1998**, *41*, 3253−3260. (c) Fedoroff, O. Y.; Salazar, M.; Han, H.; Chemeris, V. V.; Kerwin, S. M.; Hurley, L. H. *Biochemistry* **1998**, *37*, 12367−12374. (d) Perry, P. J.; Reszka, A. P.; Wood, A. A.; Read, M. A.; Gowan, S. M.; Dosanjh, H. S.; Trent, J. O.; Jenkins, T. C.; Kelland, L. R.; Neidle, S. *J. Med. Chem.* **1998**, *41*, 4873−4884.

(6) Anantha, N. V.; Azam, M.; Sheardy, R. D. *Biochemistry* **1998**, *37*, 2709−2714.

(7) Wheelhouse, R. T.; Sun, D.; Han, H.; Han, F. X.; Hurley, L. H. *J. Am. Chem. Soc.* **1998**, *120*, 3261−3262.

(8) Zahler, A. M.; Williamson, J. R.; Cech, T. R.; Prescott, D. M. *Nature* **1991**, *350*, 718−720.

(9) (a) Kim, N. W.; Piatyszek, A. M.; Prowse, K. R.; Harley, C. B.; West, M. D.; Ho, P. L. C.; Coviello, G. M.; Wright, W. E.; Weinrich, S. L.; Shay, J. W. *Science* **1994**, *266*, 2011−2015. (b) Rhyu, M. S. *J. Natl. Cancer Inst.* **1995**, *87*, 884−894. (c) Lundblad, V.; Wright, W. E. *Cell* **1996**, *87*, 369−375. (d) Holt, S. E.; Wright, W. E.; Shay, J. W. *Eur. J. Cancer* **1997**, *33*, 761−766. (e) Wright, W. E.; Tesmer, V. M.; Huffman, K. E.; Levene, S. D.; Shay, J. W. *Genes Dev.* **1997**, *11*, 2801−2809.

10.1021/ja981554t CCC: $18.00
Published on Web 02/18/1999

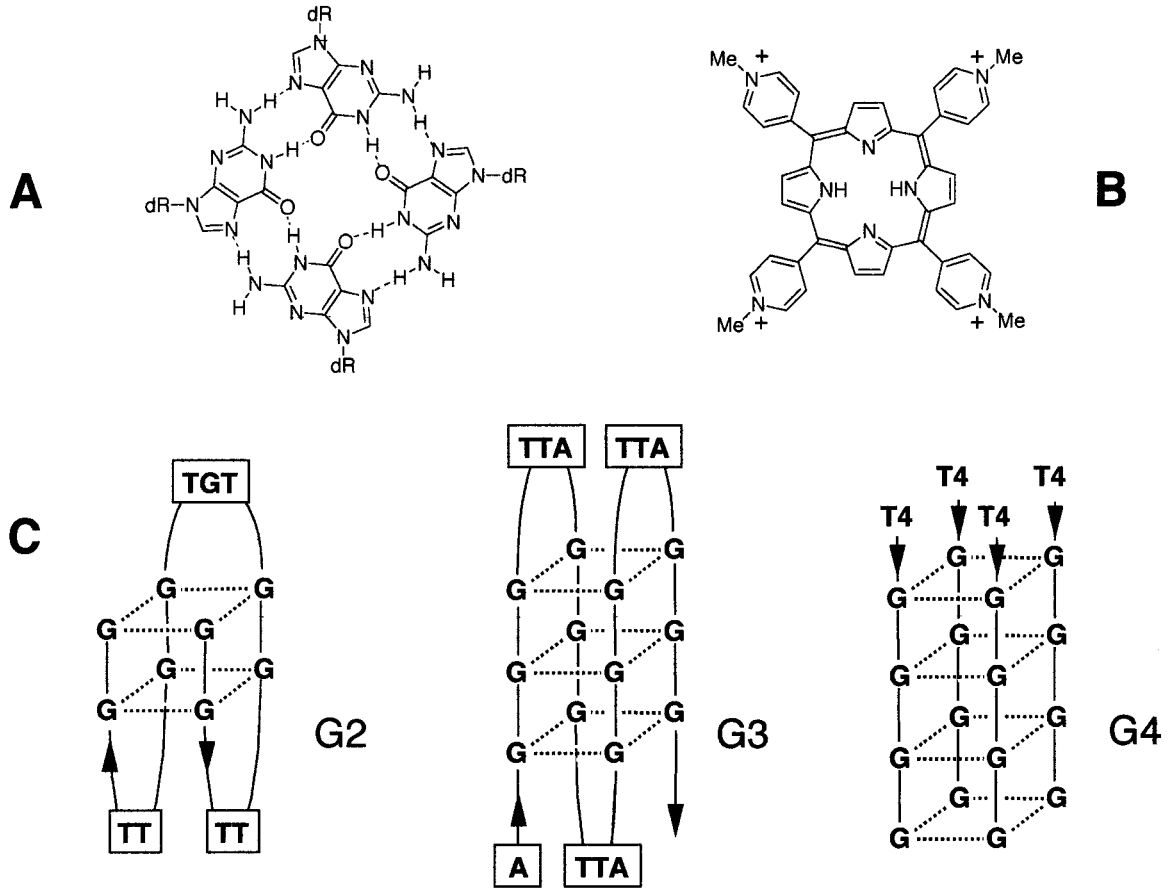

Figure 1. Structures for (A) an individual guanine base G-tetrad, showing the H-bonded planar arrangement, and (B) the H_2TMPyP cationic porphyrin used in this study. The G2 (15-mer), G3 (22-mer), and G4 (4 × 8-mer) tetraplexes examined are shown schematically (C), with the folding topologies and 5′ → 3′ strand alignments for each DNA system.

telomerase inhibitors for use as antiproliferative therapeutics and designed to target the DNA tetraplex receptor, principally either planar or "extended-planar" aromatic molecules. It has been suggested that such ligands are capable of interactive stacking with the G-tetrads present in these DNA structures (Figure 1A), by analogy with the stabilization afforded to their duplex or triplex counterparts.[5,7,10−12] In this respect, molecular tailoring methods can be used to achieve a structure-selective recognition of the tetraplex and to minimize unwanted side effects due to competitive binding to low-order DNA. Thus, for example, a series of telomere-binding anthraquinone derivatives has recently been developed where a decreased affinity for duplex DNA is suggested to be responsible for their lack of mutagenicity.[13]

Studies of the tetraplex−drug binding interactions have largely been confined to spectroscopic investigations,[5a,6,7,10−12] although a recent NMR study has provided the first structural information for complexation with a dicationic perylene derivative.[5c] However, the various findings suggested to us that this family of ligands could interact by a number of distinct mechanisms involving intercalation, end pasting or "sandwich"-type stacking, groove binding, or nonspecific external events involving charge neutralization. Binding data accumulated for this class of ligand are not unequivocal regarding the mode of interaction.

The metal-free tetracationic porphyrin H_2TMPyP (Figure 1B),[1] where the molecular dimensions resemble those of a G-tetrad,[6,7,12] was recently shown to be an effective inhibitor of human telomerase by an in vitro assay.[7] Studies of the tetraplex-binding behavior with human telomeric sequences using NMR, UV titration techniques, and an electrophoretic photocleavage assay confirmed an overall stabilization of the formed DNA complex but were not conclusive as to either the overall stoichiometry or DNA site involved.[7] In a parallel report, optical and fluorescence energy transfer studies indicated high affinity toward a parallel-stranded tetraplex, but with an unusually low binding stoichiometry.[6] Such affinity has suggested the use of this compound as a specific fluorescent probe for the detection of tetraplex DNA in situ.[12]

In the present study we examine the interactions of H_2TMPyP with three biologically relevant but distinct DNA tetraplexes (Figure 1C): the intramolecular 15-mer and 22-mer foldback structures $d(G_2T_2G_2TGTG_2T_2G_2)$ and $d(AG_3[T_2AG_3]_3)$ and the intermolecular $[d(T_4G_4)]_4$ structure formed from parallel 8-mer strands. These systems [herein denoted G2, G3, and G4] represent the DNA tetraplex structures formed by a thrombin-binding aptamer[14] and the single-stranded human[2c] and *Oxytricha*[6,11] telomeric sequences, respectively. Isothermal titration calorimetry (ITC[1]), UV absorption spectrophotometry, and molecular modeling methods are used to determine the stoichiometry and thermodynamics for binding to each DNA structure. Buffered solutions containing only either K^+ or Na^+

(10) Chen, Q.; Kuntz, T. D.; Shafer, R. H. *Proc. Natl. Acad. Sci. U.S.A.* **1996**, *93*, 2635−2639.
(11) (a) Guo, Q.; Lu, M.; Marky, L. A.; Kallenbach, N. R. *Biochemistry* **1992**, *31*, 2451−2455. (b) Lu, M.; Guo, Q.; Kallenbach, N. R. *Biochemistry* **1992**, *31*, 2455−2459.
(12) Arthanari, H.; Basu, S.; Kawano, T. L.; Bolton, P. H. *Nucleic Acids Res.* **1998**, *26*, 3724−3728.
(13) Venitt, S.; Crofton-Sleigh, C.; Agbandje, M.; Jenkins, T. C.; Neidle, S. *J. Med. Chem.* **1998**, *41*, 3748−3752.

at a fixed ionic strength (i.e., 10 mM MH_2PO_4/M_2HPO_4 + 200 mM MCl) were used to establish any dependence for binding behavior on the metal ion present to stabilize the DNA system.

The results indicate that porphyrin complexation involves an intercalative mechanism, where the stacked G-tetrad planes are inferred to provide a GpG binding site, and that high ligand/DNA loading can be realized. Importantly, the solution environment for the tetraplex has a powerful influence upon the binding behavior, such that K^+ ions produce a host DNA with degenerate sites of low affinity, whereas stepwise binding is found in Na^+-containing solutions to discrete sites with markedly different affinities. A plausible model is developed to support a binding process for the porphyrin where neighbor exclusion effects are unimportant for proximate ligand molecules at high stoichiometric loads, so that adjacent sites can be occupied simultaneously. The results provide a firm quantitative basis for the binding mechanism with this ligand and are significant for the development of superior tetraplex-stabilizing agents with potential chemotherapeutic use as antiproliferative agents or as diagnostic probes for high-order nucleic acid structures.

Experimental Section

Materials. The oligodeoxynucleotides used to prepare the G2, G3, and G4 tetraplexes [i.e., $d(G_2T_2G_2TGTG_2T_2G_2)$, $d(AG_3[T_2AG_3]_3)$, and $d(T_4G_4)$, respectively; see Figure 1C] were purchased as their HPLC-purified sodium salts from Oswel DNA Service (Southampton, Hants., U.K.). Capillary electrophoretic analysis using denaturing conditions showed each oligomer to be >99.5% homogeneous. DNA solutions were prepared in either all-potassium (K-BPES: 10 mM KH_2PO_4/K_2HPO_4, 200 mM KCl, 0.1 mM EDTA) or all-sodium (Na-BPES: 10 mM NaH_2PO_4/Na_2HPO_4, 200 mM NaCl, 0.1 mM EDTA) aqueous buffer (μ ~230 mM),[15] pH 7.00 ± 0.01, as required, and dialyzed against the same buffer for 24 h before use. Solutions were quantitated by UV spectrophotometry at 260 nm and 95 °C from extinction coefficients estimated for the single-stranded DNA species by the nearest-neighbor method,[16] using ϵ_{260} values of 1.43×10^5, 2.29×10^5, and 7.36×10^4 M(strand)$^{-1}$ cm^{-1} for $d(G_2T_2G_2TGTG_2T_2G_2)$, $d(AG_3[T_2AG_3]_3)$, and $d(T_4G_4)$, respectively. Each tetraplex was prepared by heating a solution of the appropriate DNA strand in the required buffer to 95 °C for 10 min and annealing by slow cooling to 5 °C during 48 h.

Porphyrin (H_2TMPyP: 5,10,15,20-tetrakis(1-methyl-4-pyridyl)-21*H*-porphine; Figure 1B) was purchased as the tetra-4-tosylate salt (Sigma) and used as supplied. Solutions for binding experiments were freshly prepared in the same K-BPES or Na-BPES buffer used for the DNA and quantitated by optical absorption[17] using $\epsilon_{424} = 2.26 \times 10^5$ M^{-1} cm^{-1}. Ligand solutions were kept in the dark to prevent photodegradation.

Instrumentation. Absorption spectra were recorded at 25.0 ± 0.1 °C using a Cary 1E spectrophotometer fitted with a constant temperature accessory and interfaced to an IBM 486/SX computer for data collection. Quartz cuvettes of 10 mm path length were used for all optical studies to minimize self-absorption effects. All calorimetric experiments were performed at 25.00 ± 0.01 °C using a MicroCal MCS high-sensitivity isothermal titration calorimeter (MicroCal Inc., Northampton, MA) linked to a RM PC-5200 computer for data acquisition and analysis.

Isothermal Titration Calorimetry (ITC). Calorimetric titrations were set up in K-BPES or Na-BPES buffer, as required, using DNA (G2, G3, or G4) concentrations of 40−95 μM of tetraplex in the sample cell and porphyrin ligand (titrant) concentrations of 0.5−1.0 or 3.0−3.3 mM. The higher ligand concentration was required to examine secondary binding processes in solutions containing Na^+ ions (see later), whereas this factor was unimportant for titrations in K^+ solution. The limited solubility of H_2TMPyP in the aqueous buffers thwarted the use of the ~10 mM ligand concentration judged to be optimal to define the weak secondary events. Binding isotherms were obtained by selecting the concentration of DNA titrate such that K_b·[DNA] ≥ 3−10 in all experiments, where K_b is the intrinsic equilibrium binding constant.

For a typical titration, serial 15-μL injections of ligand solution (18 aliquots) were added to the tetraplex solution at 300-s intervals. The heat output per injection was obtained by integration and correction for the sample concentration and instrument characteristics.[18] Control titrations were performed to determine the heats of dilution for each reactant, using either buffer titrated into DNA or porphyrin titrated into buffer (see later); these heat terms were subtracted from the binding heats prior to analysis.

The corrected binding isotherms were fitted to obtain the K_b value, the number of binding sites (n) per tetraplex, and the enthalpy change ($\Delta H°$) associated with the interaction, using Origin 5.0 software (MicroCal Inc., Northampton, MA) for models that assume a single set of identical binding sites.[18a] Attempted fits for models assuming either nonequivalent or competitor sites showed no statistical improvement. No constraints were placed upon the n parameter during iterative least-squares fitting; the artificial use of exact integral values (e.g., n = 1, 2, or 3) did not significantly improve the fit parameters.

Visible Absorption Spectra. Solutions of the porphyrin (10 μM) and each DNA tetraplex (100 μM of G2, G3, or G4) were prepared in K-BPES buffer. Working solutions containing a fixed concentration of porphyrin (5 μM) were prepared by mixing equal volumes of ligand solution and either buffer or DNA solution, to give mixtures with [tetraplex]/[H_2TMPyP] mole ratios of 0:1 and 10:1. Absorbance spectra were recorded in the 360−600 nm visible range, after equilibration at 25 °C for 10 min, to compare the behaviors of the free and fully bound ligands in the absence and presence of excess DNA.

Continuous Variation Analysis. Binding stoichiometries were obtained for H_2TMPyP with each of the G2, G3, and G4 tetraplexes using the method of continuous variation.[15,19] The concentrations of both ligand and DNA (in terms of whole tetraplex) were varied, while the sum of the reactant concentrations was kept constant at 5.0 μM. Solutions of H_2TMPyP (5 μM) and each annealed DNA (5 μM) were prepared in K-BPES buffer. Two series of solutions, each with 21 samples, were prepared in polystyrene cuvettes. In the sample solutions, the mole fraction χ_L of ligand was varied from 0 to 1.0 in 0.05 ratio steps by mixing χ_L mL of porphyrin solution with $(1 - \chi_L)$ mL of DNA solution, to give a final volume of 1.0 mL. Each mixture was equilibrated at 25 °C for 15 min in the dark. In the second series of blank solutions, a similar procedure was used with the DNA solution replaced by K-BPES buffer. Visible absorption spectra were recorded at 25 °C, and differential spectra were obtained after correction for the corresponding DNA-free controls. Absorbance values taken at 434−437 nm [λ_{max} for the DNA-bound porphyrin (see below)] were normalized to the maximal increase in absorbance obtained for that complex and plotted against the mole fraction of total ligand present. Binding stoichiometries were obtained from the χ_{int} intercepts after linear

(14) (a) Padmanabhan, K.; Padmanabhan, K. P.; Ferrara, J. D.; Sadler, J. E.; Tulinski, A. *J. Biol. Chem.* **1993**, *268*, 17651−17654. (b) Wang, K. Y.; McCurdy, S.; Shea, R. G.; Swaminathan, S.; Bolton, P. H. *Biochemistry* **1993**, *32*, 1899−1904. (c) Macaya, R. F.; Schultze, P.; Smith, F. W.; Feigon, J. *Proc. Natl. Acad. Sci. U.S.A.* **1993**, *90*, 3745−3749. (d) Marathias, V. M.; Wang, K. Y.; Kumar, S.; Pham, T. Q.; Swaminathan, S.; Bolton, P. H. *J. Mol. Biol.* **1996**, *260*, 378−394.

(15) Jenkins, T. C. In *Methods in Molecular Biology, Vol. 90: Drug−DNA Interaction Protocols*; Fox, K. R., Ed.; Humana Press: Totawa, 1997; pp 195−218.

(16) (a) Cantor, C. R.; Warshaw, M. W.; Shapiro, H. *Biopolymers* **1970**, *9*, 1059−1077. (b) Cantor, C. R.; Schimmel, P. R. *Biophysical Chemistry, Part III: The Behavior of Biological Macromolecules*; W. H. Freeman: New York, 1980; pp 1239−1289.

(17) (a) Pasternack, R. F.; Gibbs, E. J.; Villafranca, J. J. *Biochemistry* **1983**, *22*, 2406−2414. (b) Pasternack, R. F.; Gibbs, E. J.; Villafranca, J. J. *Biochemistry* **1983**, *22*, 5409−5417.

(18) (a) Wiseman, T.; Williston, S.; Brandts, J. F.; Lin, L. N. *Anal. Biochem.* **1989**, *179*, 131−137. (b) Ladbury, J. E.; Chowdhry, B. Z. *Chem. Biol.* **1996**, *3*, 791−801. (c) Haq, I. In *Biocalorimetry: Applications of Calorimetry in the Biological Sciences*; Ladbury, J. E., Chowdhry, B. Z., Eds.: John Wiley & Sons: Chichester, U.K., 1998; pp 41−61.

(19) (a) Job, P. *Ann. Chim. (Paris)* **1928**, *9*, 113−203. (b) Likussar, W.; Blotz, D. F. *Anal. Chem.* **1971**, *43*, 1265−1272. (c) Huang, C. Y. *Methods Enzymol.* **1982**, *87*, 509−525.

least-squares fits to the left- and right-hand portions of the Job plots using $\chi_{int}/(1 - \chi_{int})$.[15,19]

Absorbance Titration Experiments. Binding assays were performed in K-BPES buffer for all tetraplexes, and also in Na-BPES for G4, with optical monitoring at 422 nm (λ_{max} for the Soret band in the free porphyrin). The procedure is adapted from previous optical studies of DNA−ligand binding.[7,15,20] A solution of H_2TMPyP (10.0 μM) was titrated by stepwise addition of aliquots of DNA solution (1.0 mM in tetraplex) to give fixed [DNA]/[porphyrin] mole ratios in the 0−10:1 range. After each addition, the mixture was kept at 25 °C for 10 min before measurement. All readings were corrected for dilution due to the volume (≤10% max) of added DNA solution so that the total concentration of porphyrin was fixed at 10 μM throughout the experiment. Optical bleaching at 422 nm was judged complete for all samples at the 10:1 stoichiometry, indicating that the ligand is fully bound under these conditions. The fractional decrease in absorbance at 422 nm for each [DNA]/[ligand] ratio was normalized using $\Delta A = (A_{free} - A)/(A_{free} - A_{sat})$, where A_{free} and A_{sat} are the absorbances for the free and fully bound ligands (i.e., 0:1 and 10:1 mole ratios). Data from triplicate experiments were plotted versus the [tetraplex]/[H_2TMPyP] molar ratio for each DNA. The fraction of bound drug α (on a 0−1 scale) at each intermediate titration position is given directly by the relative ΔA hypochromicity term.[21] The concentration of free porphyrin is calculated using $C_f = (1 - \alpha)\cdot C$, where C is the total ligand concentration (fixed at 10 μM) and can be used to determine the binding ratio r, defined as $(C - C_f)$/[DNA]. Titration data were cast into the form of Scatchard plots of r/C_f versus r for analysis. Binding data were fitted by nonlinear least-squares analysis to a neighbor exclusion model[22] that considers occupancy of multiple binding sites:

$$r/C_f = K_i(1 - nr)[(1 - nr)/(1 - (n - 1)r)]^{n-1} \quad (1)$$

where K_i is the intrinsic equilibrium binding constant and n is an exclusion parameter that defines the number of ligand molecules bound per DNA tetraplex. Data were also fitted using the simpler, linear Scatchard equation:

$$r/C_f = K_i(n - r) \quad (2)$$

to evaluate alternative models involving identical but independent binding sites. Iterative procedures were used to obtain fits to binding data ($0.2 \geq \alpha \geq 0.8$) using the KaleidaGraph 3.08 program (Synergy Software, Reading, PA). No advantage was found using an extended form of the neighbor exclusion equation that incorporates a cooperativity factor.[15,22]

Molecular Modeling. Both intramolecular (G2) and intermolecular DNA tetraplex systems were selected for molecular modeling and energy minimization. Starting models were built using DNA coordinates reported for the chair-type folded NMR structure[14d] of d($G_2T_2G_2$-$TGTG_2T_2G_2$) and the crystal structure[2e] of $[d(TG_4T)]_4$ [Brookhaven Protein DataBase entries 1QDF and 244D]. The intermolecular parallel tetraplex was used to construct G4-type models as no structure is available for a blunt-ended DNA system. As the 5′ and 3′ thymine bases are probably involved in a π-stacked stabilization[2e,f] of the terminal G-tetrads in the $[d(TG_4T)]_4$ system, these flanking bases were included in the 5′-TGGGGT models using standard B-DNA geometries. Intercalation sites were incorporated for each tetraplex by using phosphodiester backbone parameters taken from published structures for intercalated DNA duplex−ligand complexes. A constructed model for the H_2TMPyP tetracation was optimized using the AMBER 5.0 program,[23] with appropriate force field parameters[24] and partial charges obtained from ab initio calculations at the 6-31G* level with the GAMESS package;[25] the restrained electrostatic potential fit routine[26] was used. The geometry of the resulting porphyrin closely resembled the published crystal structure.[27]

On the basis of the binding results obtained (see later), two porphyrin−G4 models were evaluated to examine possible intercalative modes: (i) the 1:1 complex TGG*GGT with a single, centrally positioned ligand (denoted *) within the G-tract core and (ii) the 3:1 complex TG*G*G*GT, where a ligand is accommodated between each pair of adjacent tetrad planes. In contrast, models for three distinct 1:1 complexes were evaluated for the folded G2 structure to compare the relative site stabilities for core- and loop-intercalated or "end-pasted" modes, denoted as 5′-*GGTT, 5′-G*GTT, and 5′-GG*TT (cf. Figure 8). Each H_2TMPyP ligand molecule was positioned in starting models to effect greatest π-overlap between the aromatic rings of the ligand and adjacent G-tetrad(s) with each DNA, but with minimal contact to bases in either loop region for the G2 complexes.

Models were hydrated in a 10 Å box of TIP3P waters using standard rules; Na^+ cations were added, and then Cl^- counterions were placed randomly for charge neutrality. Box sizes were adjusted to include 2790 waters for each model. Simulations were performed in the isothermal isobaric ensemble (300 K, 1 atm) with the AMBER 5.0 program[23] and AMBER-95 force field, using periodic boundary conditions and the particle mesh Ewald algorithm. Molecular dynamics (MD) simulations used the Sander routine (1.5-fs time step), with SHAKE to freeze all bonds involving hydrogen. All calculations were performed on a Silicon Graphics Origin 200 server and a NPACI Cray T3E (San Diego Supercomputer Center, CA). Each system was slowly heated and equilibrated for 150 ps, with gradual removal of positional restraints for the DNA and ligand.[28] Further equilibration for 200 ps, with gradual linear removal of H-bonded restraints [initially 20 kcal (mol·Å)$^{-1}$], was used to maintain the G-tetrad conformation and to prevent artifacts from the choice of starting model. After equilibration, production runs of 400 ps were used to obtain an average structure for each complex (taken from 100 snapshots accumulated in the last 100 ps), which was then fully minimized to give the final structure.

Results and Discussion

Structural Stability of the DNA Tetraplexes. Previous studies have shown that the association process to form a four-stranded DNA is kinetically slow.[29] Thus, the G2, G3, and G4 structures were prepared in aqueous solution at pH 7.0 from heat-denatured solutions by slow annealing during 48 h to maximize their formation. Two buffer systems of fixed ionic strength ($\mu \sim 230$ mM), K-BPES and Na-BPES, differing only in the presence of either K^+ or Na^+, were used to examine the effect of the monovalent cation upon any binding behavior.

After preparation, all DNA solutions were assessed by parallel differential scanning calorimetry (DSC) and UV thermal

(20) Pasternack, R. F.; Garrity, P.; Ehrlich, B.; Davis, C. B.; Gibbs, E. J.; Orloff, G.; Giartosio, A.; Turano, C. *Nucleic Acids Res.* **1986**, *14*, 5919−5931.

(21) Peacocke, A. R.; Skerrett, J. N. H. *J. Chem. Soc., Faraday Trans.* **1956**, *52*, 261−279.

(22) McGhee, J. D.; von Hippel, P. H. *J. Mol. Biol.* **1974**, *86*, 469−489.

(23) Cornell, W. D.; Cieplak, P.; Bayly, I.; Gould, I. R.; Merz, K. M.; Ferguson, D. M.; Spellmeyer, D. C.; Fox, F.; Caldwell, J. W.; Kollman, P. A. *J. Am. Chem. Soc.* **1995**, *117*, 5179−5197.

(24) AMBER parameters for the porphyrin molecule were adapted from Giammona, D. A. Ph.D. Thesis, University of California, Davis, CA, 1984; see http://www.amber.ucsf.edu/amber/ff94/contrib/heme/frcmod.hemall.

(25) Schmidt, M. W.; Baldridge, K. K.; Boatz, J. A.; Elbert, S. T.; Gordon, M. S.; Jensen, J. J.; Koseki, S.; Matsunaga, N.; Nguyen, K. A.; Su, S.; Windus, T. L.; Dupuis, M.; Montgomery, J. A. *J. Comput. Chem.* **1993**, *14*, 1347−1363.

(26) (a) Bayly, C. I.; Cieplak, P.; Cornell, W. D.; Kollman, P. A. *J. Phys. Chem.* **1993**, *97*, 10269−10280. (b) Cornell, W. D.; Cieplak, P.; Bayly, C. I.; Kollman, P. A. *J. Am. Chem. Soc.* **1993**, *115*, 9620−9631.

(27) Ford, K. G.; Pearl, L. H.; Neidle, S. *Nucleic Acids Res.* **1987**, *15*, 6553−6562.

(28) The stepwise modeling protocol used is (i) energy minimize waters only, (ii) 25 ps MD at 100 K, holding both DNA and H_2TMPyP with a restraint of 100 kcal (mol·Å)$^{-1}$, (iii) re-minimize waters, (iv) minimize whole system, (v) 25 ps MD at 100 K, holding DNA/H_2TMPyP [100 kcal (mol·Å)$^{-1}$], and (vi) five sequential 25 ps MD steps at 300 K, with a gradual loosening of restraints for DNA/H_2TMPyP [i.e., 100, 50, 25, 5, and 0.5 kcal (mol·Å)$^{-1}$]. This procedure was used to obtain the models required for further MD simulations, after thermal equilibration at 300 K using H-bonded restraints.

(29) (a) Williamson, J. R. *Annu. Rev. Biophys. Biomol. Struct.* **1994**, *23*, 703−730. (b) Wyatt, J. R.; Davis, P. W.; Freier, S. M. *Biochemistry* **1996**, *35*, 8002−8008.

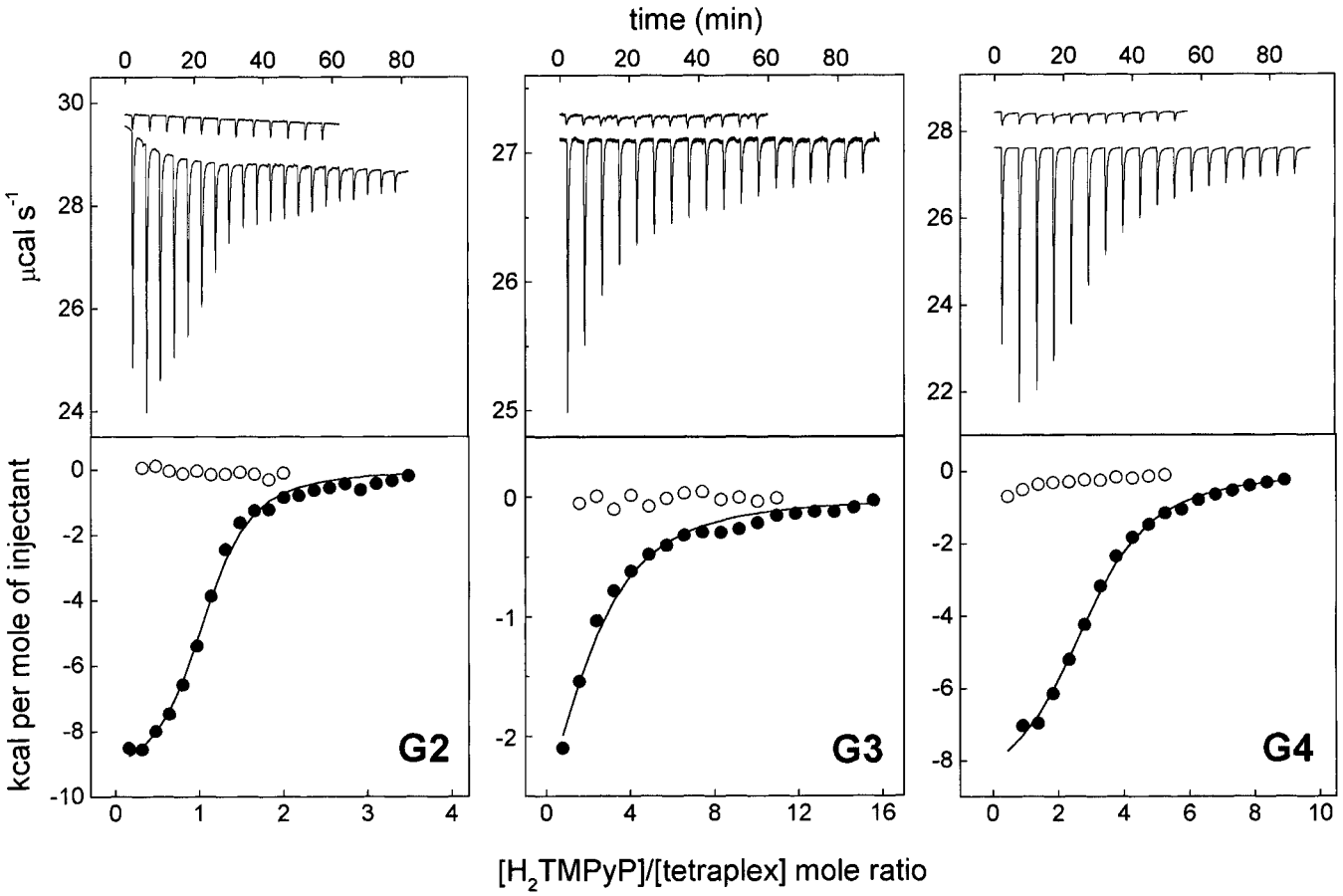

Figure 2. Raw calorimetric data (upper panels) for titration of either aqueous K-BPES buffer or a DNA solution (42−94 μM G2, G3, or G4 tetraplex) with serial injections of H_2TMPyP solution (15-μL aliquots of 0.5−1.0 mM) at 25 °C, showing exothermic binding and ligand dilution processes. The *y*-axis represents the cell feedback energy response to maintain a constant temperature. Fitted binding isotherms (lower panels) as a function of [ligand]/[DNA] molar ratio for each DNA system, showing stoichiometries of 1:1 for G2, 2:1 for G3, and 3:1 for G4 at the turnover points (○, buffer alone; ●, DNA). In each case, the corrected experimental heats were fitted using a model that assumed a single set of identical binding sites (see text).

denaturation experiments before use. Such studies are a vital prerequisite for thermodynamic binding studies[18c,30] to ensure that experiments are performed below the melting temperature (T_m) of the relevant DNA species. Thermal transitions were typically 10−20 °C higher for DNA solutions in the all-K^+ buffer compared to the equivalent all-sodium buffer, with T_m values >45 °C (i.e., 53 °C for G2, 73 °C for G3, and 49 °C for G4). Both G3 and G4 gave broad optical melting transitions (not shown) at 4 μM(tetraplex) in K-BPES or B-BPES solutions, with only modest ~7% hyperchromicity at 260 nm, but melting could not be reliably established for the G2 DNA in either buffer, as noted previously.[14b] DSC experiments at higher DNA concentrations (100−400 μM) typical of those used in our ITC studies showed thermal behaviors in good agreement with the optical melts, together with T_m data for the G2 tetraplex. The results are consistent with earlier reports for these and related DNA tetraplexes using spectroscopic and calorimetric techniques.[11b,14b,c,31] In particular, the melting properties of the thrombin-binding G2 aptamer in K^+ and Na^+ solution are in accord with those of an independent DSC study.[14c]

Tetraplex stabilization by monovalent metal ions has been discussed extensively, with the $K^+ > Na^+$ quantitative rank order for preference interpreted in terms of a superior fit to the central cavities of the planar G-tetrads. Thus, the assembly of G-rich DNA sequences to form a tetraplex is favored under high-[K^+] conditions.[2c,11,31] As all optical and calorimetric binding experiments in the present study were performed at 25 °C, the DNA hosts used are assumed to be predominantly in their respective tetraplex forms in the presence of each cation at this ionic strength (~215 mM K^+ or Na^+). However, as the T_m for denaturation of G2 in the Na^+ buffer occurs at only 35−40 °C, we would expect this DNA to be appreciably single-stranded under the all-sodium Na-BPES conditions used.

Isothermal Titration Calorimetry (ITC). ITC is a sensitive technique for probing bimolecular processes and can provide direct information about the binding affinity and stoichiometry and the key thermodynamic parameters involved.[18] The interactions of H_2TMPyP with the intramolecular foldback G2 and G3 tetraplexes, and with the intermolecular G4 tetraplex (Figure 1C), were examined at 25 °C using all-K^+ (K-BPES) and all-Na^+ (Na-BPES) buffered conditions.

Figure 2 shows the results of calorimetric titrations for the interactions of H_2TMPyP with the three DNA tetraplexes in K-BPES buffer. Primary calorimetric data are shown for titration of the ligand into buffer or buffered DNA solution (heat peaks in upper panels). Integration of the heats produced per injection, with respect to time, and conversion to a per mole basis gives the corresponding binding isotherm (lower panels). The binding data must be corrected for the dilution heats associated with

(30) (a) Haq, I.; Ladbury, J. E.; Chowdhry, B. Z.; Jenkins, T. C. *J. Am. Chem. Soc.* **1996**, *118*, 10693−10701. (b) Haq, I.; Ladbury, J. E.; Chowdhry, B. Z.; Jenkins T. C.; Chaires, J. B. *J. Mol. Biol.* **1997**, *271*, 244−257.

(31) (a) Jin, R.; Gaffney, B. L.; Wang, C.; Jones, R. A.; Breslauer, K. J. *Proc. Natl. Acad. Sci. U.S.A.* **1992**, *89*, 8832−8836. (b) Pilch, D. S.; Plum, G. E.; Breslauer, K. J. *Curr. Opin. Struct. Biol.* **1995**, *5*, 334−342. (c) Miura, T.; Benevides, J. M.; Thomas, G. J. *J. Mol. Biol.* **1995**, *248*, 233−238.

each reactant, separately determined by injection of either (i) buffer into DNA solution or (ii) ligand solution into buffer.

In a series of control experiments, the heat of dilution for each tetraplex was found to be constant and negligible for the 40−100 μM range used. In contrast, dilution of the H_2TMPyP ligand was moderately exothermic but independent of concentration in the 0.1−3 mM range (in either buffer), becoming essentially thermoneutral only at concentrations near 5 mM that approach the solubility limit. On this basis, and the fact that the ligand obeys Beer's law (0−15 μM range) in both buffers, we judge the porphyrin to be essentially monomeric at the concentrations used in our ITC experiments. This conclusion agrees with a recent NMR study of porphyrin self-association showing that aggregation or dimerization effects are not significant at concentrations up to 1 mM.[32]

After correction for dilution effects with each reactant, the heat data were fitted using a model that assumes a single set of identical binding sites to determine the stoichiometry *n*, binding constant K_b, and interaction enthalpy $\Delta H°$ parameters.[18a] Superior fits could not be obtained for models involving either nonequivalent or multiple interacting competitor sites; indeed, attempted fits to such alternative models were always considerably poorer. The thermodynamic parameters determined from the optimal fits (lower panels in Figure 2) for repeat experiments at 25 °C in K^+ solution are collected in Table 1.

Calorimetric Data in K^+ Solution. The binding data obtained by ITC in K-BPES buffer (Table 1) show an affinity order of G2 > G4 ≫ G3 for the porphyrin and that all interactions are exothermic. Table 1 reveals that distinct binding stoichiometries of 1:1, 2:1, and 3:1 H_2TMPyP molecules per tetraplex are obtained for the G2, G3, and G4 structures in solutions containing 200 mM K^+ (actually ∼215 mM including the buffering components). These results contrast with a value of ∼0.6:1 for porphyrin−G4 binding reported from a spectrophotometric analysis using different buffer conditions (100 mM TRIS-borate/100 mM K^+/20 mM Mg^{2+}, pH 8.0)[6] but agree with a 2:1 value determined for the human G3 sequence (50 mM sodium phosphate/100 mM NaCl, pH 7.0) from an independent optical study.[7] We note that the earlier G4 study was carried out in the presence of Mg^{2+}, which has been shown to have unfavorable effects on tetraplex formation,[33] suggesting that the different solution conditions used may, in part, be responsible for the altered ratio. The low stoichiometry for porphyrin−G4 resulted from a Scatchard fit to experimental data with binding ratios *r* in a 0.35−0.55 range; such a narrow range may be insufficient to reliably estimate binding parameters by extrapolation (also see below).[15,22] However, we note that 1:1 binding stoichiometries have been determined by ITC for other ligands with the G3 and G4 tetraplexes[5d,11a] and by optical titration for a dicarbocyanine dye with a dimeric hairpin tetraplex,[10] although a wide range of buffer and salt conditions were used in these studies. The present study is the first report to compare the thermodynamic binding behavior of a ligand with a series of tetraplexes using defined solution conditions.

Binding to each DNA is characterized by weak affinities of (3−20) × 10^4 M^{-1} per binding site which only just exceed the lower limit detectable by the ITC method (Table 1).[18] These values disagree with a 2.7 × 10^7 M^{-1} value reported from Scatchard analysis of porphyrin−G4 complexation[6] but compare favorably with a value of 1.5 × 10^5 M^{-1} for the corresponding complex with ethidium bromide,[11a] (5−8) × 10^4 M^{-1} for

Table 1. Parameters for Porphyrin Binding to the G2, G3, and G4 DNA Tetraplexes,[a] Obtained by ITC and Optical Titration at 25 °C

host DNA	calorimetric data				optical data (Scatchard)[b]			optical data (N. E.)[c]		
	n[d]	K_b ($\times 10^4$ M^{-1})	$\Delta H°$ (kcal mol^{-1})	$\Delta G°$ (kcal mol^{-1})	$T·\Delta S°$ (kcal mol^{-1})	n[d]	K_i ($\times 10^4$ M^{-1})	r	n[d]	K_i ($\times 10^4$ M^{-1})	r
K^+ buffer:[e]											
G2	1.0 ± 0.0	17.8 ± 2.3	−9.6 ± 0.2	−7.2 ± 0.1	−2.4 ± 0.3	1.2 ± 0.1	22.0 ± 4.1	0.92	0.9 ± 0.1	25.1 ± 2.3	0.91
G3	1.9 ± 0.4	2.8 ± 0.7	−4.2 ± 0.8	−6.1 ± 0.1	+1.9 ± 0.8	1.8 ± 0.2	7.4 ± 0.9	0.95			
G4	2.9 ± 0.1	7.7 ± 0.8	−9.1 ± 0.3	−6.7 ± 0.1	−2.4 ± 0.3	2.6 ± 0.2	17.0 ± 1.5	0.98			
Na^+ buffer:[e]											
G2	*f*	*f*	*f*			nd	nd		nd	nd	
G3−1	1.1 ± 0.0	3.3 ± 0.3	−6.8 ± 0.2	−6.2 ± 0.1	−0.6 ± 0.2	nd	nd		nd	nd	
G3−2	1.0 ± 0.2[g]	∼0.2 ± 0.4[g]	∼ −6[g]								
G4−1	1.1 ± 0.0	162 ± 18	−6.7 ± 0.0	−8.5 ± 0.1	+1.8 ± 0.1	0.9 ± 0.1	423 ± 68	0.95	1.1 ± 0.1	407 ± 51	0.94
G4−2	2.0 ± 0.1	4.4 ± 0.6	−25.3 ± 1.1	−6.3 ± 0.1	−19.0 ± 1.1						

[a] G2, G3, and G4 refer to $d(G_2T_2G_2TGTG_2T_2G_2)$, $d(AG_3[T_2AG_3]_3)$, and $[d(T_4G_4)]_4$, respectively (cf. Figure 1C). Thermodynamic parameters were calculated using the standard relationships $\Delta G° = -RT·\ln K_b = \Delta H° - T·\Delta S°$. [b] Data fit using the Scatchard model (eq 2). [c] Data fit using the neighbor exclusion model (eq 1). [d] Number of ligand molecules bound per tetraplex at saturation. [e] Determined in K-BPES (K^+) or Na-BPES (Na^+) buffer, pH 7.0, containing 200 mM KCl or NaCl. [f] No resolvable binding isotherm was obtained. [g] Saturation of weak secondary binding prevented by porphyrin insolubility. nd = not determined. The *r* values shown represent correlation coefficients for the optical data fits.

(32) Kano, K.; Minamizono, H.; Kitae, T.; Negi, S. *J. Phys. Chem. A* **1997**, *101*, 6118−6124 (and references therein).

(33) Ross, W. S.; Hardin, C. C. *J. Am. Chem. Soc.* **1994**, *116*, 6070−6080.

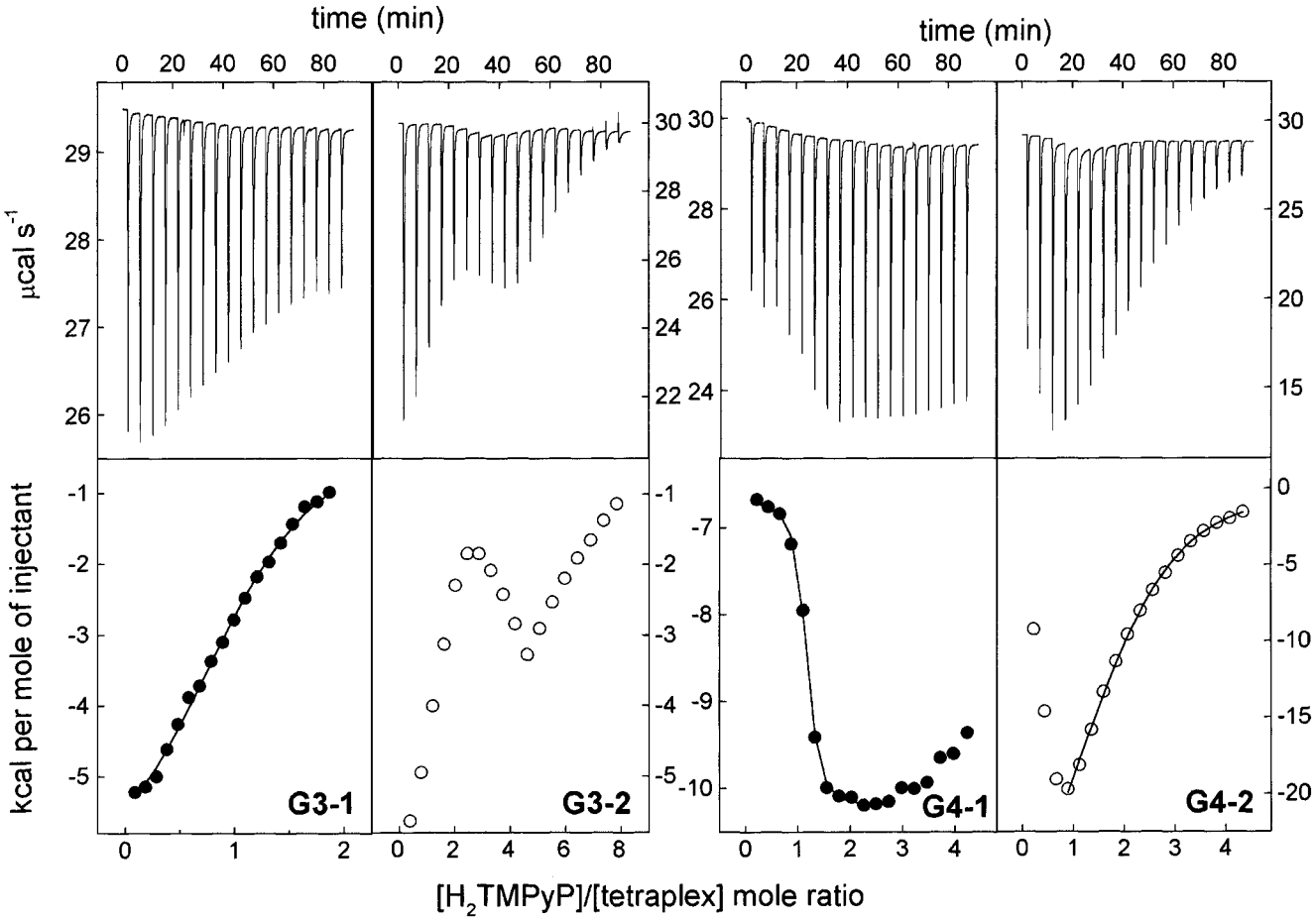

Figure 3. Raw calorimetric data (upper panels) for titration of a DNA solution in Na-BPES buffer (82−87 μM G3 or G4) with serial injections of porphyrin solution [15-μL aliquots of 0.9 mM (left, first event) or 3.0−3.3 mM (right, second event)] at 25 °C, showing the exothermic behaviors. Fitted isotherms (lower panels) as a function of [ligand]/[DNA] molar ratio, showing stoichiometries of 1:1 for each initial binding event (denoted as G3−1 or G4−1) and 2:1 for the subsequent G4−2 binding. The second binding process for G3 (i.e., G3−2) could not be fully fitted as saturation is not possible due to the limiting concentrations for the reactants. All interaction heats are corrected for dilution effects.

anthraquinone−G3 binding,[5d] and values of 10^4−10^6 M^{-1} for the binding of a series of fused-ring polycyclic acridines to tetraplexes derived from the human telomere sequence (Dr. E. Giménez-Arnau, personal communication).

Calorimetric Data in Na^+ Solution. Figure 3 shows the results of parallel ITC titrations for the interactions of H_2TMPyP with the DNA tetraplexes in Na-BPES buffer. Calorimetric data are shown for titration of the ligand into buffered solutions of G3 and G4 (heat peaks in upper panels), together with the corrected binding isotherms (lower panels). The binding behaviors in the Na^+ buffer were found to be considerably different compared to the equivalent K^+ solutions, with a sequential accumulation of ligand to sites of different affinity and/or stoichiometry. Thus, the interactions with G3 and G4 are characterized by a high-affinity initial binding event, requiring only low [H_2TMPyP]/[DNA] ratios to effect saturation, followed by a weaker, secondary process that requires a much higher ligand concentration to achieve saturation. To optimize the ITC response[18] and thereby distinguish each event, titrations of the G3 and G4 DNA tetraplexes (80−90 μM) were carried out with porphyrin concentrations of 0.5−1.0 mM for the first step (denoted G3−1 and G4−1) and 3.0−3.3 mM for the second steps (denoted G3−2 and G4−2), respectively (Figure 3). Saturation of the G3−2 binding event, and hence a fully resolved isotherm, was prevented by limited solubility for the porphyrin in the Na-BPES buffer, estimated to require 5−10 mM. No reproducible isotherm could be obtained for the G2 tetraplex using any combination of reactant concentration, suggesting either poor affinity or that the DNA structure is unstable at 25 °C under the Na^+ conditions used. The melting behavior determined for G2 in Na-BPES (see above) is consistent with thermodynamic instability of the host tetraplex.

The isotherms obtained for the interaction processes in Na-BPES solution, each fitted assuming a single set of identical binding sites, are shown in Figure 3 (lower panels) and the determined parameters are collected in Table 1. The results show that the overall binding stoichiometries are unaltered for solutions containing Na^+ instead of K^+, although the 2:1 value for G3 (i.e., stepwise 0:1 → 1:1 → 2:1) and the 3:1 value for G4 (i.e., stepwise 0:1 → 1:1 → 3:1) indicate that the sites involved must be distinct and no longer degenerate. It is notable that the equilibrium constant for the initial G3/4−1 event is ∼20−40-fold greater than that for the secondary G3/4−2 event(s). Further, the affinity of the parallel-stranded G4 tetraplex toward the porphyrin is greatly enhanced in the presence of Na^+ ions, such that the first binding process dominates the overall profile for interaction.

Optical Binding Studies. Figure 4 shows the visible absorption spectra of the porphyrin in the all-potassium K-BPES buffer in the absence or presence of the G2, G3, and G4 tetraplexes. In each case, marked changes are evident in the spectral behavior of the ligand for both the intense Soret band at 422 nm and the weaker absorption at 518 nm. The induced bathochromic red-shifts and hypochromicities for the Soret band are consistent

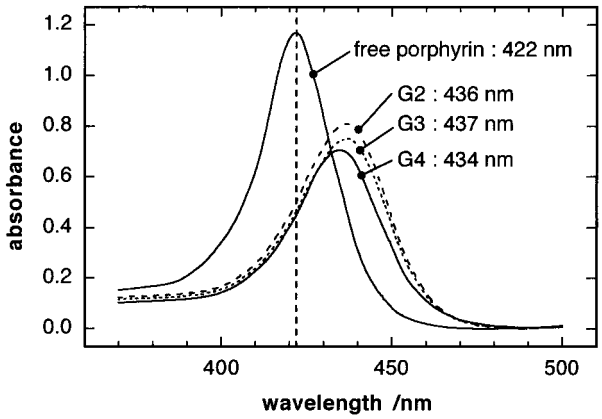

Figure 4. Visible absorbance spectra of H_2TMPyP in the absence and presence of the G4, G3, or G2 DNA tetraplex in K-BPES solution at 25 °C for a constant porphyrin concentration of 5.0 μM. A fixed [tetraplex]/[H_2TMPyP] molar ratio of 10:1 was used to compare the free and fully bound ligands. The binding-induced red shifts and hypochromicities, relative to the Soret band at 422 nm, are +14 nm (31%) for G2, +15 nm (36%) for G3, and +13 nm (40%) for G4. Qualitatively similar effects (not shown) are induced for the weaker porphyrin absorption at 518 nm (free ligand), with red-shifts of +8 nm (G2), +8 nm (G3), and +6 nm (G4). The Soret band used to monitor free ligand in the binding analyses is indicated.

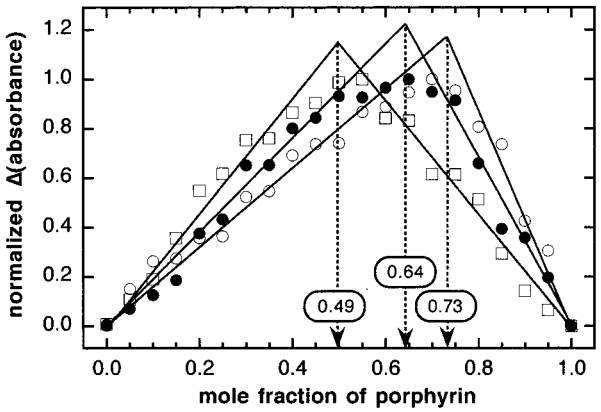

Figure 5. Job plots for the binding of H_2TMPyP to the G2 (□), G3 (●), and G4 (○) tetraplexes in K-BPES buffer solution at 25 °C. The sum of the porphyrin and DNA tetraplex concentrations was fixed at 5 μM. Optical absorbance changes for the bound porphyrin at 436 nm (G2), 437 nm (G3), or 434 nm (G4) are normalized to the maximum increase in each case. The *y*-axis represents the difference in absorbance for mole fractions of ligand (χ_L) in DNA and in buffer alone. Intercept mole fraction values were determined from least-squares fits to the linear data portions, giving χ_{int} values of 0.49 (1.0:1 stoichiometry) for G2, 0.64 (1.8:1) for G3, and 0.73 (2.7:1 stoichiometry) for G4, respectively.

with spectral changes reported previously for porphyrin−tetraplex binding[6,7,12] in buffered solutions containing Na^+, K^+, or Na^+/K^+ mixtures. Such effects are indicative of binding and can be used to characterize the DNA−ligand complexation using quantitative spectrophotometric techniques [for a recent review, see ref 15].

Binding of H_2TMPyP to G2, G3, and G4 was first examined at 25 °C in K-BPES buffer by the method of continuous variation to determine the overall stoichiometries. In each case, the progressive increase in absorption at 434−437 nm for the DNA-bound ligand was monitored as a function of mole fraction of added porphyrin (at a fixed summed concentration of 5.0 μM for the reactants). Figure 5 shows normalized Job plots for each DNA, with intercept mole fraction values χ_{int} of 0.49 (G2), 0.64 (G3), and 0.73 (G4) that correspond to porphyrin/tetraplex

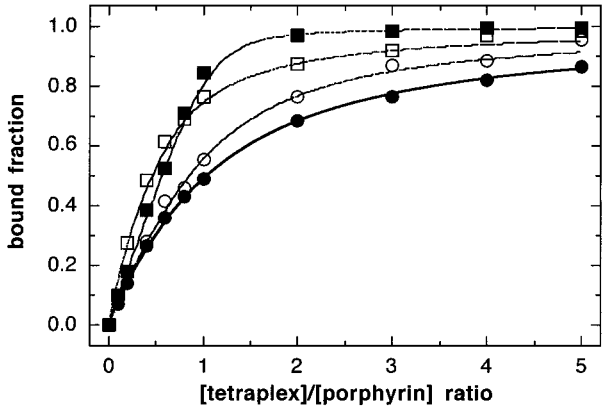

Figure 6. Bleaching plots for titration of H_2TMPyP (10 μM) at 25 °C with the G2 (○), G3 (●), and G4 (□) tetraplexes in K-BPES buffer, or with G4 in Na-BPES buffer (■). The fraction of bound porphyrin is given by the binding-induced decrease in absorbance at 422 nm for each [DNA]/[ligand] ratio, after normalizing to the optical change for the free and fully bound ligands at ratios of 0:1 and 10:1. The data are consistent with binding constants of $\sim 10^5$ M^{-1} in the K^+ buffer and reveal an increased affinity for G4 in the presence of Na^+ ions. Fitted parameters to the Scatchard or neighbor exclusion binding models (see text) are listed in Table 1. The curves shown represent the optimal Scatchard fits.

stoichiometries of 1.0:1, 1.8:1, and 2.7:1, respectively. These values confirm the saturating stoichiometries determined by direct ITC titration (Table 1) in K^+ buffer. Interestingly, the ~2:1 ratio determined for the foldback G3 tetraplex is identical to that reported from a Job study in an all-Na^+ buffer, in accord with the ligand load determined to exert a maximal hypochromic shift for the porphyrin Soret band.[7] The small curvature evident in Figure 5 for each Job plot is consistent with K_b values of $\sim 10^5$ M^{-1} for binding (i.e., $1/K_d < 5$ μM).[19c] Solutions of the porphyrin (10 μM) were also titrated by stepwise addition of the G2, G3, or G4 tetraplex (each 1 mM in whole tetraplex) to construct Scatchard equilibrium binding plots in K^+ buffer. For comparison, the experiment with G4 was also repeated using the analogous Na^+ buffer. The loss of absorbance or bleaching at 422 nm during titration, corresponding to a progressive removal of free porphyrin (Figure 4), was used to determine the equilibrium position relative to the free and fully bound ligands. The fraction of drug bound at each titration position was then plotted versus the [DNA]/[H_2TMPyP] molar ratio to give the optical binding isotherm (Figure 6). This procedure is analogous to that used by Pasternack and colleagues to examine porphyrin−DNA binding and suggested[20] to avoid bias in any subsequent model-based data fitting.

Table 1 shows the results from Scatchard analysis of the optical data for a simple model involving independent identical binding sites (eq 2); fitted theoretical curves are shown in Figure 6 for the experimental data. Alternative binding analysis using the neighbor exclusion model (eq 1) for multiple sites were indistinguishable (Table 1) from the Scatchard fits for G2 in K^+ and for G4 in Na^+. The bleaching data show a clear rank order for binding given by G4 (Na^+) ≫ G2 > G4 (K^+) > G3. Further, the stoichiometries and binding constants obtained by titration in K^+-containing solution agree with the values determined by direct ITC measurement, although the K_i values appear to be ~3-fold greater than their K_b counterparts. The parameters for the G4 DNA indicate that porphyrin binding is 25-fold stronger in solutions with Na^+ ions, such that a switch occurs from the 3:1 binding found in K^+ solution to an apparent 1:1 stoichiometry (see below).

These optical experiments confirm the ligand-binding stoichiometries and affinities for each tetraplex obtained by ITC, particularly in solutions containing K^+ ions, and further illustrate that the behavior is greatly influenced by the solution conditions.

Degenerate Intercalative Binding of the Stacked G-Tetrads. Direct measurement of the binding enthalpies (Table 1) shows that the interactions of H_2TMPyP with each tetraplex are enthalpically driven under the K^+ solution conditions used. The major enthalpic binding forces are countered by a small unfavorable entropic term for G2 and G4, whereas the entropic $T\cdot\Delta S°$ contribution for G3 instead favors binding, although the resulting $\Delta G°$ values are closely similar. Such effects may partly reflect inherent differences in hydration for the DNA structures and/or binding-induced release of counterions. Thus, for example, a larger entropic term due to release of condensed counterions could be expected for the porphyrin−G4 complex because of the greater binding load achievable with the tetracationic ligand. Structural factors involving accessibility and any binding-induced rearrangement or distortion must also be important. Interestingly, these thermodynamic parameters resemble those reported using ITC for binding of ethidium bromide to the G4 tetraplex (i.e., $\Delta H° = -5.9$ kcal mol^{-1}, $T\cdot\Delta S° = +1.4$ kcal mol^{-1}, and $\Delta G° = -7.3$ kcal mol^{-1})[11a] and for binding of two isomeric anthraquinone derivatives to the G3 structure (i.e., $\Delta H° = -5.5/-10.1$ kcal mol^{-1}, $T\cdot\Delta S° = +1.2/-3.7$ kcal mol^{-1}, and $\Delta G° = -6.7/-6.4$ kcal mol^{-1}),[5d] suggesting that qualitatively similar mechanisms may be involved.

Previous calorimetric studies[20] with double-stranded calf thymus DNA at 25 °C report $\Delta H°$ values of −4.6, −5.9, and +1.5 kcal mol^{-1} for H_2TMPyP and the metalated derivatives CuTMPyP and ZnTMPyP, respectively. Binding for H_2TMPyP and the Cu(II) derivative is interpreted in terms of intercalation of the DNA duplex at G/C sites,[20,34a] whereas the Zn(II) complex is nonintercalating and instead binds through possible groove- or outside-mediated mechanisms, or by spear-type modes.[6,20,34] The similarity between the enthalpic terms for porphyrin intercalation and H_2TMPyP−tetraplex binding suggests that analogous binding is probably involved. In this respect, the $\Delta H°$ values per site are also typical for intercalative ligand binding to duplex and triplex DNA.[30a,35] Intercalation would be consistent with reported fluorescence energy transfer and hypochromism studies for the porphyrin−G4 system,[6] but differ with conclusions inferred from a photocleavage assay that implicate end π-stacking to the foldback G3 human telomere sequence.[7] A further sandwich-type binding mode has been proposed,[6] where a porphyrin is clamped in a tail-to-tail fashion between the 3′-end tetrads of two distinct tetraplexes. Quantitative support for such a mechanism has been obtained from a structural report for complexation of a dicationic perylene with a blunt-ended parallel tetraplex, although threading intercalation was found for equivalent structures with longer 3′-terminated strands.[5c]

The DNA tetraplexes used in this study differ primarily in that their structures contain two (G2), three (G3), or four (G4) stacked G-tetrad planes, respectively (Figure 1C).[2c,6,11,14] The ITC and optical results obtained in K^+ solution reveal stoichiometries of 1:1, 2:1, and 3:1 for these host tetraplexes, with degenerate or closely equivalent binding sites for both the G3 and G4 DNA systems. Examination of Figure 1C suggests that this behavior could be consistent with ligand intercalation between each pair of successive G-tetrad planes in the DNA structures. Intriguingly, the stoichiometries for each DNA tetraplex correspond exactly to the number of potential intercalation sites provided by the stacked G-tetrads. However, simultaneous occupation of adjacent GpG intercalation sites in these DNA hosts would require that neighbor exclusion effects do not dictate the recognition and binding events. The distal positive charges of a DNA-bound porphyrin would be expected to interact favorably with the backbone phosphates, whereas bulk or steric contact between bound ligands (e.g., through the pyridinium groups in the grooves) could be detrimental for accommodation of a proximate molecule.

Considering the G4 system, it is evident that a fully intercalated 5′-TG*G*G*G model, where the asterisks represent a ligand bound at each GpG site, would satisfy the experimental binding data. Alternative arrangements involving end-stacked 5′-T*GGGG or "end-pasted" 5′-TGGGG* ligands are possible, involving TpG intercalation or single-sided interaction between the ligand and the blunt 3′ end of the G-tetrad stack, but clearly at least one porphyrin must be accommodated by threading through the core region of the tetraplex to satisfy the observed 3:1 stoichiometry. An end-pasted molecule would stabilize the complex by π-stacking with the adjacent tetrad, as has been suggested to prevent "end fraying" of a tetraplex by a flanking nucleotide base.[11b] However, it is unlikely that the sites implicated in any 3:1 mixed-mode organization of ligands could be viewed as equivalent as contrasting affinities would be expected for the disparate sites.

Similarly, a 5′-AG*G*GT model would satisfy the 2:1 degenerate binding behavior for the intramolecularly folded G3 system, although end-stacked 5′-A*G or 5′-T*G competitor modes involving intercalation of the diagonal and parallel loop regions can also be realized. In contrast, three distinct binding models can be envisaged for the foldback G2 aptamer system: 5′-*GGTT, 5′-G*GTT, and 5′-GG*TT, corresponding to end-pasted, core-intercalated, and loop-intercalated modes, respectively (cf. Figure 8).

Clearly, it is not possible to distinguish possible modes from the available ITC and optical data alone, but the similarity for binding behaviors obtained with the otherwise unrelated DNA structures provides compelling support for an intercalative mechanism. In the absence of detailed structural information for a complex, the only reliable criterion for DNA intercalation would normally involve the use of hydrodynamic techniques.[36] However, while such methods may be useful to examine the stoichiometry in the present context it is unlikely, as the effects upon helical length would be similar, that the binding sites involved could be established.

Molecular modeling techniques provide a ready means to assess both the feasibility of intercalative binding and the effects of increasing ligand load upon the DNA complexation. To this end we have embarked upon a qualitative examination of the π-stacking processes through which a porphyrin can be accommodated by host DNA tetraplexes, where a primary aim is to compare end-stacked, end-pasted, and core-intercalated binding modes.

Molecular Models for Tetraplex Binding. Preliminary molecular dynamics modeling studies of intercalated complexes support the conclusions from our biophysical data for binding. Two distinct DNA systems were selected to examine possible intercalative modes for the H_2TMPyP ligand, involving (i) 1:1

(34) (a) Lipscomb, L. A.; Zhou, F. X.; Presnell, S. R.; Woo, R. J.; Peek, M. E.; Plaskon, R. R.; Williams, L. D. *Biochemistry* **1996**, *35*, 2818−2823. (b) Pasternack, R. F.; Gibbs, E. J. In *Metal Ions in Biological Systems*; Siegel, A., Sigel, H., Eds.: Marcel Dekker: New York, 1997; pp 367−397.

(35) (a) Hopkins, H. P.; Fumero, J.; Wilson, W. D. *Biopolymers* **1990**, *29*, 445−459. (b) Chaires, J. B.; Priebe, W.; Graves, D. E.; Burke, T. G. *J. Am. Chem. Soc.* **1993**, *115*, 5360−5364.

(36) Suh, D.; Chaires, J. B. *Bioorg. Med. Chem.* **1995**, *3*, 723−728.

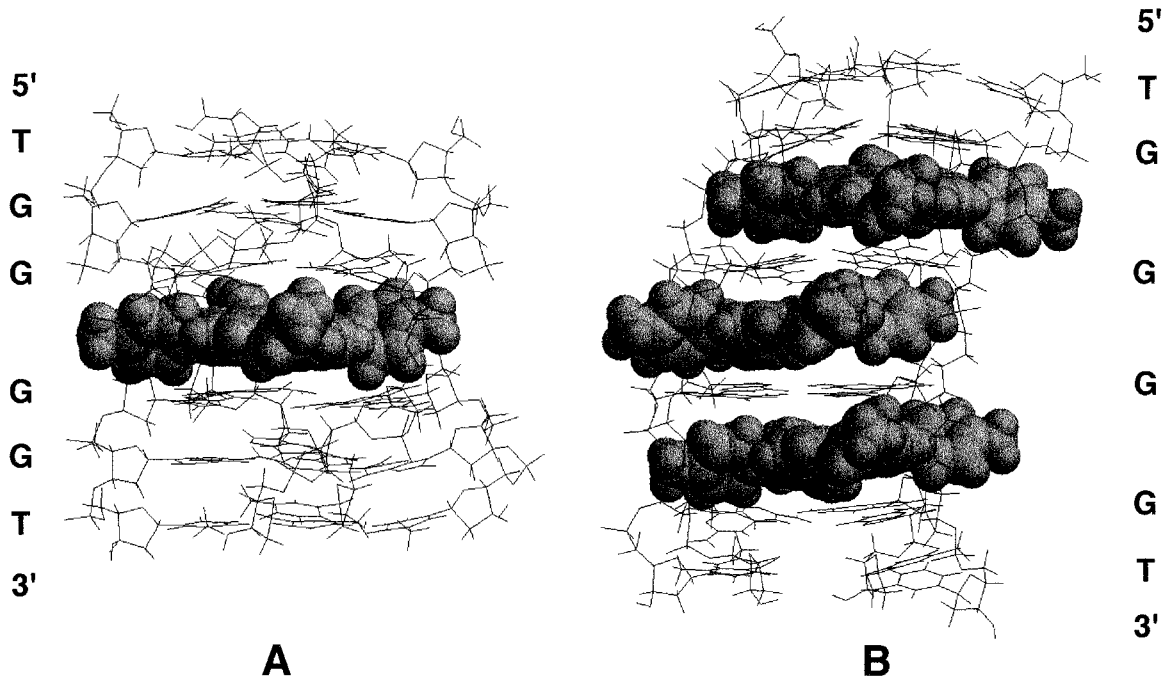

Figure 7. Energy-minimized structures for possible intercalation of the $[d(TG_4T)]_4$ tetraplex with (A) 5′-TGG*GGT (1:1 binding) and (B) 5′-TG*G*G*GT (3:1 binding), where each asterisk denotes a H_2TMPyP ligand. The complexes are viewed looking toward the G-tetrad stack with the porphyrin(s) shown in space-fill mode. Note the axial offset of the porphyrin relative to the long helical axis in the 1:1 core-intercalated complex and the alternating pattern of ligand displacements in the 3:1 complex.

binding to the folded intramolecular G2 tetraplex and (ii) 1:1 and 3:1 binding to the intermolecular $[d(TGGGGT)]_4$ tetraplex. The latter parallel system was used to enable a comparison with the G4 structure as structural data are unavailable for an intermolecular tetraplex with blunt-end strands (see the Experimental Section).

Energy minimization resulted in stable structures for all complexes examined with the DNA tetraplexes. A major finding is that the planar H_2TMPyP ligand molecule can be intercalated within the $d(TG_4T)_4$ and G2 structures to stabilize the complex through favorable π-stacked interactions between aromatic residues, as for "classical" duplex intercalation, but without significant disruption of the guanine tetrads.

Figure 7A shows the stable 1:1 core-intercalated complex with the $[d(TG_4T)_4]_4$ tetraplex, 5′-TGG*GGT, after refinement as described. Examination of the model shows that the ligand adopts a parallel alignment between the successive tetrad planes with the molecule displaced asymmetrically from the DNA helical axis. The ligand is offset so that two of the noncoplanar 1-methylpyridinium groups effectively protrude into adjacent groove conduits of the tetraplex. As a consequence, the two other substituent rings do not extend as far into their respective DNA grooves and are drawn toward the intercalation site, thereby inducing a minor perturbation of the local tetrad planarity. This result suggests that the extended planar ring system of the porphyrin is actually smaller than a G-tetrad and hence cannot effect a simultaneous equivalent π-stabilization of all four guanine bases in the array. Sliding-type rearrangement or dynamic relocation of the porphyrin would be expected to stabilize the entire tetrad in each plane, although this was not seen in the production-run time scale (400 ps) used for our simulations. The binding process requires a change of local DNA conformation to accommodate the porphyrin, so that the phosphate backbone is linearized relative to that of the B-type DNA host and the tetrad planes implicated are rotated to a more superimposable alignment (Figure 7A). However, such conformational effects are not propagated extensively, as the overall integrity of the tetraplex is retained and the structure remains stable throughout the dynamic simulation.

The core-intercalated 5′-TGG*GGT model complex is well behaved and remains stable after inclusion of further porphyrin molecules between the adjacent stacked G-tetrads to achieve higher stoichiometric ratios. Figure 7B shows the 3:1 complex 5′-TG*G*G*GT after minimization, showing the axial or slipped displacement of each H_2TMPyP ligand and the alternating groove protrusion for each successive ligand. Such asymmetric binding results in an effective removal of interligand contacts and is suggested to diminish the influence of neighbor exclusion upon binding stoichiometry and/or increased ligand load. The structure for the 3:1 complex illustrates the binding-induced linearization afforded to the DNA backbone and confirms an effective coplanarity and retention of stacking for both the ligand and G-tetrad systems. Further molecular modeling is in progress to examine alternative end-stacked or end-pasted arrangements (e.g., 5′-T*GGGGT and 5′-TGGGG*) and to establish the influence of flanking 5′ and 3′ bases upon the stability of the complexes. Analyses of the dynamic behaviors, energies, and structures will be detailed elsewhere.

More extensive simulations were carried out for the three possible 1:1 intercalated d(**GGTT**GGTGTGGTTGG)−H_2TMPyP complexes to probe site-dependent binding effects. The averaged trajectory energies after MD equilibration showed that the 5′-G*GTT model for intercalation of the core G-tract is more stable than either alternative end-pasted 5′-*GGTT or intercalated ("end-stacked") 5′-GG*TT models involving the different loop regions of the host G2 tetraplex (cf. Figure 1C). The time-averaged structure for each complex was stripped of water and counterions and then subjected to a full refinement procedure (see Experimental Section). Comparison of energies for the minimized structures revealed that the 5′-G*GTT complex (Figure 8B) is considerably more favorable than the 5′-*GGTT (Figure 8A) or 5′-GG*TT (Figure 8C) complexes, with relative energies of 0, +140, and +250 kcal mol^{-1}, respectively. This ranking order reflects differences in π-overlap for the G-tetrad

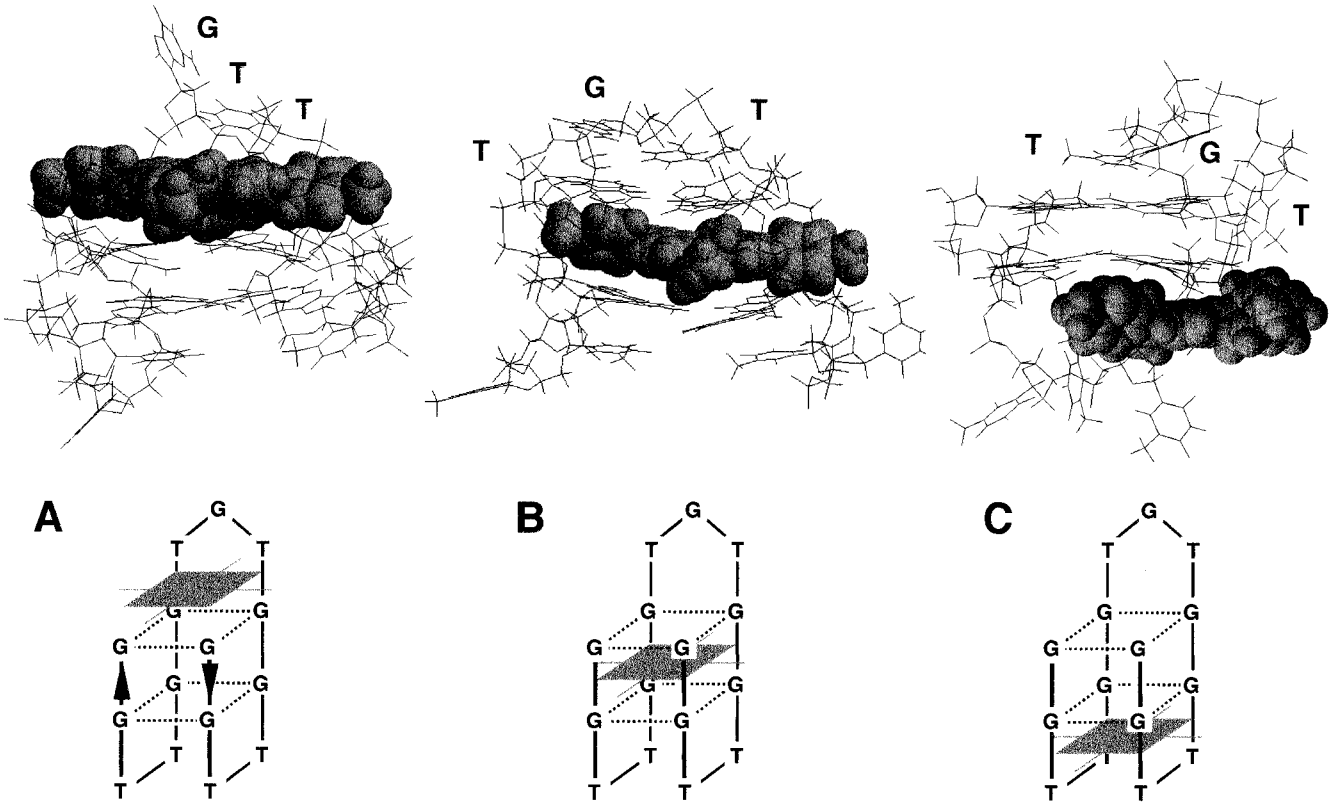

Figure 8. Energy-minimized structures for three 1:1 intercalated porphyrin−G2 complexes with (A) 5′-*GGTT, (B) 5′-G*GTT, and (C) 5′-GG*TT, where the asterisk denotes the H_2TMPyP molecule. Each complex is viewed looking toward the stacked G-tetrads, with the TGT loop in the folded tetraplex as indicated and the ligands shown in space-fill mode. The schematic diagrams indicate the strand directions in the host tetraplex and the alignments for the tetrad and ligand planes in each complex. The order for stabilization is 5′-G*GTT > 5′-*GGTT > 5′-GG*TT (relative energies of 0, +140, and +250 kcal mol^{-1}), showing that binding between two G-tetrads (model B) is more favorable than either "end-pasting" (model A) or loop intercalation (model C), where only a single G-tetrad is implicated.

and porphyrin ring systems, disturbance of favorable 5′/3′-end stacking from the loop thymines, and disruption of the guanine quartets by the porphyrin substituents due to asymmetric positioning of the ligand (see above). Thus, the H_2TMPyP molecule in the 5′-GG*TT complex (Figure 8C) moved considerably from the initial docked position to give a structure where π-overlap is achieved with only two guanines in the adjacent tetrad. Such a lateral displacement results in spear rather than full intercalation in the TT loop region, and hence a poorer binding energy. In contrast, significantly greater π-overlap is achieved for the 5′-*GGTT complex involving the less sterically crowded TGT loop region of the structure.

Taken together these modeling results support the conclusions from the ITC and optical data and demonstrate that intercalation of both inter- and intramolecular tetraplexes can result in stable DNA−porphyrin complexes. Further studies are required to assess the effects of increased ligand load (i.e., higher stoichiometry) upon the site specificity and structural integrity. To this end, we recently examined the stabilization of the folded G3 human tetraplex by a series of isomeric anthraquinones using a less extended modeling protocol.[5d] This study culminated in a model for complexation with the ligand intercalated at the 5′-A*G step that accounts for the 1:1 binding stoichiometry established using ITC. Given that we find a 2:1 stoichiometry for porphyrin binding to the same G3 structure in both K^+ and Na^+ buffer, it is likely that factors such as sequence context and ligand complexion may govern the site specificity and/or ultimate stoichiometry. This conclusion is supported by the distinct stoichiometries established from an NMR binding study of a perylene ligand to intermolecular tetraplexes with blunt-ended or capped G-tract strands, resulting in 5′-TTAGGG* and 5′-(T)TAGGG*TT(A) complexes, respectively.[5c] The bulky substituents attached to the planar chromophore of this ligand would be predicted to influence any binding mechanism where groove accommodation is compromised.

Binding Involves Nonequivalent Sites in the Presence of Na^+ Ions. The calorimetric experiments reveal a dramatic alteration in binding behavior for the DNA tetraplexes toward the porphyrin upon switching from an all-K^+ buffer to a buffer of identical ionic strength but containing only Na^+ metal ions (Table 1 and Figures 2−3). While the overall stoichiometries are unaffected, provided that thermodynamic stability is retained by the DNA host in the presence of Na^+, the binding sites become nondegenerate and of different affinity. This results in stepwise binding 0:1 → 1:1 → 2:1 for G3 and 0:1 → 1:1 → 3:1 for G4, where the first ligand is ∼20−40-fold more tightly bound than any subsequent porphyrin molecule(s). In the case of the intermolecular parallel G4 tetraplex, the ITC and optical data indicate that binding is ∼25-fold stronger in the presence of Na^+ rather than K^+, such that the behavior is overwhelmed by an "apparent" 1:1 stoichiometry. Indeed, the weaker secondary binding events are effectively masked and become significant only if high concentrations of ligand are used in the experiments.

The thermodynamic parameters (Table 1) for the initial binding events in the presence of Na^+ (G3−1 and G4−1, respectively) resemble those obtained for the degenerate modes with K^+, suggesting that intercalation is similarly implicated. Full analysis for the secondary G4−2 process, thwarted for G3−2 due to practical considerations, shows a large unfavorable entropy term for acceptance of each ligand such that complexation is enthalpy−entropy compensated. This would imply that

secondary binding incurs an entropic penalty, presumably due to energetically adverse processes that stem from formation of the initial 1:1 complex.

The reason for the differential binding behavior with Na^+ is not understood but may relate to changes in inherent stability for the host DNA molecules. Tetraplex stabilization is more effective with K^+ than Na^+, such that this factor has a major influence upon the structure and thermodynamic stability,[2c,11,31] leading to conformational polymorphism in certain cases.[31c] It is likely that the G-tetrads at each end of a tetraplex formed from G-tract DNA strands may stack less effectively or have increased dynamic mobility in Na^+ solution, leading to a gradient in character for the GpG sites reading through the stack. Thus, a central intercalation site could be envisaged to have greater stability than "equivalent" sites nearer the strand termini and hence result in a favored interaction and lower stoichiometry. In contrast, the superior stabilization afforded by K^+ ions may lead to a more closely similar series of GpG sites that would result in degenerate binding. The present binding data support this view, but information from further DNA tetraplex systems (e.g., with longer G_n tracts) is clearly required to establish whether such effects are universal.

Conclusions

In summary, the present calorimetric and optical studies indicate that the cationic H_2TMPyP porphyrin binds to DNA tetraplexes by intercalation and that the saturating stoichiometry appears to correlate with the number of stacked G-tetrad planes in the host structures. Intercalative binding of ligand at these GpG sites, rather than competitive modes involving pasting or stacking to either end of the tetraplex, is supported by molecular modeling of the possible complexes. The finding that near-equivalent DNA sites are involved implies that mixed-mode binding is unlikely. However, simultaneous occupation of adjacent intercalation sites in the DNA requires that neighbor exclusion phenomena are not important for this ligand. A plausible model is developed where ligands can be closely accommodated in the complex by asymmetric positioning of successive porphyrins, without either significant interligand contact or disruption of the global tetraplex integrity. In this respect, the relatively small steric profile presented by the four attached symmetric substituents is suggested to be a significant factor in the efficiency of this porphyrin as a probe ligand for tetraplex systems.

Importantly, it is clear that the interactions are manifestly influenced by the solution conditions used for experiments, such that the degenerate binding found in the presence of K^+ for closely equivalent sites becomes nondegenerate in the presence of Na^+ ions. The binding stoichiometry is not altered using Na^+ conditions, but differential sites for stepwise binding become apparent, where an initial 1:1 high-affinity event dominates the overall interaction and masks the subsequent uptake of further ligand. To some extent this may explain the apparent disparity for reported porphyrin−tetraplex binding behaviors,[6,7] as markedly different buffer and K^+/Na^+ conditions systems were used to stabilize the DNA structures in the earlier studies. The present data establish the role of metal ions in determining the binding properties and highlight that care should be taken in comparative studies of candidate molecules designed as tetraplex-specific ligands.

The results from this study provide insight to the stabilizing behaviors and mechanism of binding for such ligands toward DNA systems. This information will assist the rational design of improved or next-generation compounds as potential inhibitors of telomerase activity, where four-stranded DNA tetraplex structures are implicated as a therapeutic target.

Acknowledgment. This work was supported by Enzacta Ltd. (T.C.J.) and the University of Greenwich (RAE Award to B.Z.C.). We thank Dr. R. T. Wheelhouse (University of Bradford) for helpful discussions and acknowledge the computational support of the NSF NPACI Supercomputing facilities (to J.O.T.).

JA981554T